Hindawi Publishing Corporation
Advances in Meteorology
Volume 2014, Article ID 581756, 11 pages
http://dx.doi.org/10.1155/2014/581756

Research Article

Uncertainty Assessment: Reservoir Inflow Forecasting with Ensemble Precipitation Forecasts and HEC-HMS

Sheng-Chi Yang and Tsun-Hua Yang

Taiwan Typhoon and Flood Research Institute, National Applied Research Laboratories, 11 F, No. 97, Section 1, Roosevelt Road, Zhongzheng District, Taipei 10093, Taiwan

Correspondence should be addressed to Tsun-Hua Yang; tshyang@narlabs.org.tw

Received 3 June 2014; Revised 1 August 2014; Accepted 4 August 2014; Published 27 August 2014

Academic Editor: Hann-Ming H. Juang

During an extreme event, having accurate inflow forecasting with enough lead time helps reservoir operators decrease the impact of floods downstream. Furthermore, being able to efficiently operate reservoirs could help maximize flood protection while saving water for drier times of the year. This study combines ensemble quantitative precipitation forecasts and a hydrological model to provide a 3-day reservoir inflow in the Shihmen Reservoir, Taiwan. A total of six historical typhoons were used for model calibration, validation, and application. An understanding of cascaded uncertainties from the numerical weather model through the hydrological model is necessary for a better use for forecasting. This study thus conducted an assessment of forecast uncertainty on magnitude and timing of peak and cumulative inflows. It found that using the ensemble-mean had less uncertainty than randomly selecting individual member. The inflow forecasts with shorter length of cumulative time had a higher uncertainty. The results showed that using the ensemble precipitation forecasts with the hydrological model would have the advantage of extra lead time and serve as a valuable reference for operating reservoirs.

1. Introduction

The available records from 1958 to 2010 show that on average 29.2 typhoons form per year, but only 3.4 affect Taiwan. Taiwan experiences multiple typhoons annually because the island is located in the path of northwest Pacific typhoons [1]. Typhoon-induced rainfall causes severe casualties and an annual average loss of more than 500 million US dollars [2]. To mitigate the typhoon impacts, reservoirs serve as an important hydraulic structure to manage flood water release at opportune times to decrease the downstream flood risk. Although Taiwan's average annual rainfall is 2.5 times more than the world's average, but the available rain water is only one-seventh of the world average. Eighty percent of precipitation is because of typhoons and storms from May to October [3]. Storing reservoir inflows during a typhoon period for future uses is imperative due to limited water resources in Taiwan.

The average impact duration of a typhoon is 73.68 h in Taiwan based on 38 historical typhoon durations from 2000 to 2009 [4]. Three days (72 h) of reservoir inflow forecasting would help decision makers optimally operate reservoirs to achieve the following purposes: first is to mitigate the downstream flood risk and second is to store available water for drier times. Applying observations from rainfall gauges can provide 0 to 3 h lead time which is insufficient for reservoir operators to take preventive measures. In addition, the failure of onsite instrumentation is always a concern during an extreme event. Other techniques, the so-called data-driven models such as artificial neural network (ANN) and autoregressive models, are also used for rainfall-runoff estimations and forecasts (e.g., [5–7]). Cheng et al. [5] concluded that the ANN model can give good prediction performance in the long-term flow discharge to a reservoir. However, the quantity and quality of data are important for these models' performance [6]. The forecast uncertainty increases if data-driven models without good data are used. High quality and quantity data are not easily collected and thus data-driven models are not considered in this study.

As an operational system, coupling numerical weather predictions (NWP) with a hydrological model at catchment scale is a straightforward strategy to provide reservoir inflow

forecasts with enough lead time. However, there are significant uncertainties associated with a hydrometeorological forecast system, including uncertainties in boundary and initial conditions and hydrological model parameters [8–10]. Rainfall forecasts as input to a hydrometeorological forecast system are the main one among all sources of uncertainty [10, 11]. Because of incomplete observations, approximate forecast models due to unavoidable simplifications, random errors from initial atmospheric conditions perturbing, and model parameterizations, the NWP model would generate different rainfall forecasts at the same location and time [9, 12]. Wilks [13] explained that different rainfall forecasts are not unpredictable or void of information, but rather not precisely predictable. The abovementioned studies confirm that the atmosphere is a nonlinear and complex system and accurate prediction is impossible [14]. The ensemble predicting system (EPS), a collection of two or more NWP forecasts at the same time, is frequently used instead of a single deterministic model to capture rainfall forecasting uncertainties [15]. It consists of an adequate number of equally likely (equiprobable) NWP models and provides probabilistic precipitation forecasts. Most weather services, such as the European Centre for Medium Range Weather (ECMWF), Swedish Hydro-Meteorological Service, and US National Weather Service (NOAA), routinely use ensemble weather predictions as inputs to operational and preoperational forecasting systems [15]. Van Steenbergen and Willems [16] addressed that EPS can cover the uncertainty produced from the rainfall forecasts of NWP models, which is one part of the integral uncertainty. It implied that the uncertainty of rainfall forecast is inevitable and the length of lead time is another cause. Other than the uncertainty from NWP models, a few studies assessed the impact of uncertainty in hydrological simulations. For example, Knighton et al. [17] used a Monte Carlo analysis to evaluate the parameters' impacts in model results' sensitivity. The uncertainty can be quantified by generating a large number of possible outcomes under given constraints. However, some studies indicated that there is less uncertainty in hydrological models parameterization than in climate models (e.g., [18–20]).

This paper intends to provide valuable information for decision makers during typhoons by considering the integral uncertainty and the length of lead time. The integral uncertainty is a combined result of all sources of uncertainty that are occurring and propagating in the forecasting process [10]. This study coupled HEC-HMS with Taiwan cooperative precipitation ensemble forecast experiment (TAPEX) to provide three days of reservoir inflow forecasts. TAPEX is a collective effort among academic institutes and government agencies in Taiwan since 2010. It aims to provide typhoon track and rainfall forecasts [1, 21] using EPS. The Shihmen Reservoir in northern Taiwan was selected as the study area. Figure 1 shows that all typhoon tracks affected Taiwan according to the historical data [4]. Among ten categories, type 2 has the most impact on the reservoir. In addition, a type 3 typhoon in 2009, named Morakot, caused Taiwan huge losses. To consider the biggest impact on the reservoir, a total of six typhoons of types 2 and 3 were selected to calibrate the system and test the performance. All the members of TAPEX produced rainfall forecasts and the ground observations model calculated the rainfalls to reservoir inflows. The integral uncertainties for magnitude and timing of peak flow and cumulative reservoir inflow were assessed and discussed.

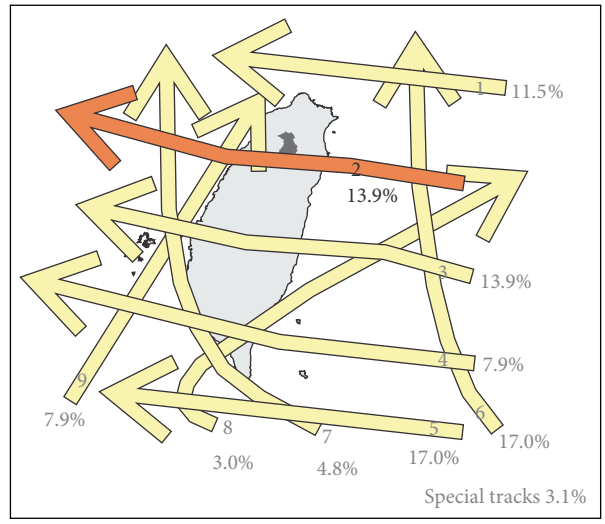

Redrawn from Kuo et al. (2012)

Figure 1: Schematic diagram of typhoon tracks invading Taiwan. The percentages in the figure were the statistic results from 1958 through 2006 by the Central Weather Bureau (CWB). The dark grey polygon located in the northern Taiwan indicates the Shihmen Reservoir catchment. Typhoons in type 2 would pass through the Shihmen Reservoir catchment and bring heavy rainfall, such as Typhoon Saola in 2012 or Typhoon Soulik in 2013.

2. Study Area

The Shihmen Reservoir catchment, located at the upstream of the Tanshui River in northern Taiwan, was selected as the study area (Figure 2). The Shihmen Reservoir is a multiple-purpose reservoir, including irrigation, water supply, flood control, hydropower, and recreation. It has a 761.05 square kilometers (km^2) catchment area and 233 million cubic meters (m^3) of effective storage capacity, which ranks the first and third among all reservoirs in Taiwan, respectively. More than two million households across 27 villages and towns in three counties rely on its water supply. In addition, one-third of the total population of the Taipei metropolitan area, the largest one in Taiwan, is downstream. It is also a part of the Taipei Flood Prevention System, a project that took 37 years to complete starting in 1963 to mitigate downstream flood risks. However, Shih et al. [22] mentioned that the vulnerability to 200-year flooding still exists due to urban development and natural alteration over time [22]. Therefore, flood control through reservoir operations is very important for downstream flood mitigation during typhoons. To achieve these two goals of water supply and flood mitigation at the same time, the operator must be precise when releasing flood waters.

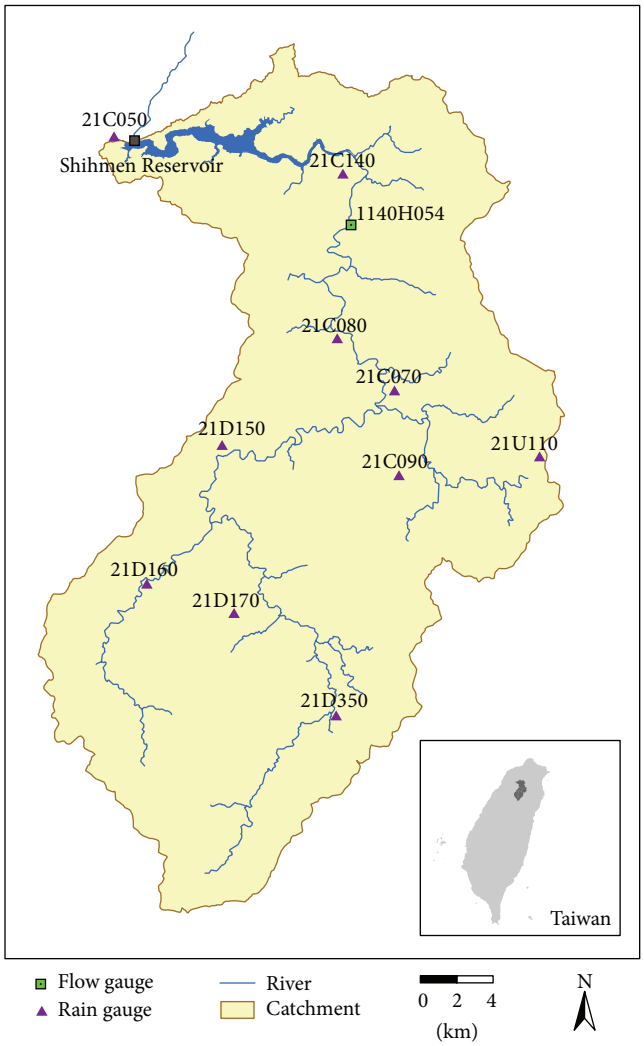

Figure 2: Study area and location of streamflow and precipitation gauges.

3. Method and Materials

This study's process consisted of three steps: data acquisition, hydrological model establishment, and error estimation (Figure 3). The observed information was used for model calibration and validation. Using TAPEX's ensemble rainfall forecasts as input, the hydrological model was calibrated using three typhoons and simulated reservoir inflows against the remaining three typhoons' observations. The error estimations of peak flow and cumulative inflow were applied to evaluate model performance. The details of the study process are described as follows.

3.1. Data Acquisition

3.1.1. Taiwan Cooperative Precipitation Ensemble Forecast Experiment (TAPEX). TAPEX, a collective effort among academic institutes and government agencies, such as National Taiwan University, National Central University, National Taiwan Normal University, Chinese Culture University, Central Weather Bureau (CWB), National Center for High-Performance Computing, Taiwan Typhoon and Flood Research Institute, and National Science and Technology Center for Disaster Reduction, started in 2010 and is the first attempt to design a high-resolution numerical ensemble model in Taiwan. The TAPEX applied various models, including the weather research and forecasting (WRF), model, the fifth-generation Penn State/NCAR mesoscale model (MM5), and cloud-resolving storm simulator (CReSS), and initial conditions for precipitation forecast. The observed data gathered worldwide from satellites, radar, atmospheric sounding, and ground observations are used in these numerical weather models (members). The experiment aims to provide 24, 48, and 72 h ensemble quantitative precipitation forecasts and generate four runs a day at a 5 km resolution. The ensemble statistical method and probabilistic forecast concept are used to analyze the typhoon path and precipitation distribution. The average (or weighted combination) of all members was used as the final precipitation forecast. For further details, please see Hsiao et al. [21] and Lee et al. [1].

3.1.2. Observed Precipitation Information. Among ten categories of typhoon invading Taiwan (Figure 1), types 1 through 5 are west-moving path typhoons, types 6 and 7 are north-moving path typhoons, type 8 is the recurving northeastward typhoon, and type 9 is the typhoon which invades Taiwan in a straight line after forming in the South China Sea. Other special typhoon tracks/paths that do not belong to any of above are called type 10. Among all the types, type 2 would pass through the Shihmen Reservoir and bring heavy rainfall on the reservoir catchment. For examples, Typhoon Saola in 2012 and Soulik in 2013 pulled down approximately 300 mm in 24 h and the observed peak inflow to the reservoir was over 5,300 cubic meters per second (m^3/s).

To characterize the biggest impact on the Shihmen Reservoir, the typhoons in type 2 were studied. This study applied the most recent typhoons, Saola (2012) and Soulik (2013), to test the system performance. Typhoon Morakot in 2009 (Type 3), causing enormous damages in Taiwan, was also selected as an extra test. The model establishment used three typhoons, Sinlaku (Type 2), Jangmi (Type 2), and Fungwong (Type 3), consistent with the abovementioned types. Table 1 lists the details of the six historical typhoons used in this study. Because of the advantages of fast computation and high calculation accuracy, Thiessen's polygon method has been widely applied [23] and was used to calculate the average rainfall (P_{ave}) as follows:

$$P_{\text{ave}} = \sum_{i=1}^{n} w_i P_i, \qquad \sum_{i=1}^{n} w_i = 1, \tag{1}$$

where P_i and w_i are the observed rainfall information and weighting factor for the ith rainfall station, respectively, and n represents a total of rainfall gaging stations. Observations with an hourly resolution provided from ten rainfall gauge

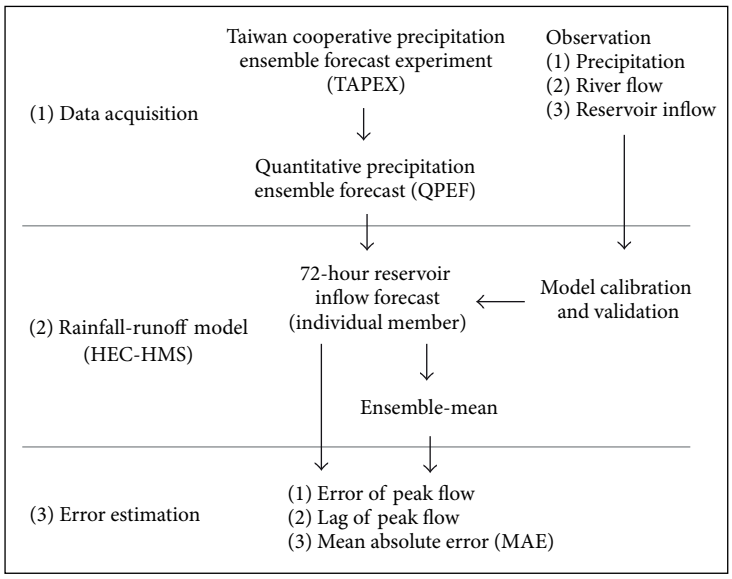

Figure 3: Flow chart of this study in terms of data processing and performance evaluation.

Table 1: Collected six typhoons' historical data. The first three typhoons' observed data, namely, Typhoon Fungwong, Typhoon Sinlaku, and Typhoon Jangmi, were used for model calibration and validation. The second three typhoons' TAPEX ensemble quantitative precipitation forecasts, namely, Typhoon Morakot, Typhoon Saola, and Typhoon Soulik, were used for model application to provide the reservoir inflow forecast for the Shihmen Reservoir.

Typhoon	Year	TAPEX period (land warning period*)	Track	Max. cumulative rainfall** (mm)		
				24 h	48 h	72 h
Fungwong	2008	— (7/27 2:30~7/29 11:30)	3	235.8	280.4	282.1
Sinlaku	2008	— (9/12 5:30~9/15 20:30)	2	412.0	711.1	899.0
Jangmi	2008	— (9/27 8:30~9/29 17:30)	2	317.2	369.2	404.4
Morakot	2009	8/6 8:00–8/8 2:00 (8/6 8:30~8/10 5:30)	3	265.0	413.3	466.7
Saola	2012	7/31 8:00–8/1 20:00 (7/31 20:30~8/3 14:30)	2	397.7	398.6	422.6
Soulik	2013	7/11 8:00–7/12 20:00 (7/11 20:30~7/13 23:30)	2	494.3	672.7	798.9

*The land waning period of typhoons was based on the Typhoon Database of Central Weather Bureau, Taiwan (http://rdc28.cwb.gov.tw/). Periods are MM/DD notation.
**Data from the Shihmen Reservoir Management Center (http://www.wranb.gov.tw/). Thiessen's polygon method was used to calculate the average rainfall and maximum cumulative rainfall. Selected precipitation gauges and the corresponding weights of Thiessen's polygon were listed in Table 3.

stations were used to calculate the average rainfall as hydrological input ($i = 1, 2, \ldots, 10$). The TAPEX generated the ten stations' rainfall forecasts to replace observations in this study. Figure 2 shows the location of these gaging stations.

3.1.3. Observed Inflow Information. The observed inflow data were collected from the Shihmen Reservoir Management Office at the Hsiayun flow gauge station (1140H054 in Figure 2). The station is located at the upstream of Shihmen Reservoir and is not affected by backwater. The data for reservoir inflow estimated by the Shihmen Reservoir Management Office during the last three typhoons in Table 1 were collected for model applications.

3.2. Rainfall-Runoff Model. HEC-HMS is a well-known hydrologic modeling software developed by the US Army Corps of Engineers (USACE) Hydrologic Engineering Center (HEC). It aims to simulate the precipitation runoff processes of watershed systems and includes different components such as runoff volume, baseflow, and channel flow. Storage and movement of water vertically within the soil layer are not included. Many studies have applied HEC-HMS for rainfall-runoff at watershed scale (e.g., [24, 25]). It is appropriate in

this study since the movements within soil are assumed to be negligible during typhoons. For each component, HEC-HMS includes many different modules. The details of HEC-HMS are given in the Technical Reference Manual [26] and User's Manual [27]. The loss is subtracted from the precipitation depth and the remaining depth is referred to as precipitation excess. In the study, soil conservation service curve number (SCS-CN) loss method was selected to estimate cumulative losses. This method estimates precipitation excess as a function of cumulative precipitation, soil cover, land use, and antecedent moisture using the following equation [26]:

$$P_e = \frac{(P - 0.2S)^2}{P + 0.8S}, \tag{2}$$

where P_e and P are cumulative precipitation excess and rainfall depth at time t; S is potential maximum retention, a measure of the ability of a watershed to abstract and retain storm precipitation. The maximum retention S is determined using the following equation (SI unit):

$$S = \frac{25400 - 254\text{CN}}{\text{CN}}, \tag{3}$$

where CN is the SCS curve number which can be estimated as a function of land use, soil type, and antecedent watershed moisture.

The value of CN is an empirical index which ranges from 100 (for water bodies) to 30 for permeable soils with high infiltration rates. In the study, the value of CN was initially based on the soil type and land use of the catchment and refinements were made during the calibration and validation process. HEC-HMS transforms the rainfall excess (P_e) to direct surface runoff through an empirical model (unit hydrograph) or a conceptual model (kinematic wave). In the study, the SCS unit hydrograph (SCS-UH) method was applied for estimating direct runoff. Research by the SCS suggests that the UH peak (U_P) and time of UH peak (T_P) are related as

$$U_P = C\frac{A}{T_P}, \tag{4}$$

where A is the watershed area; C is a conversion constant (2.08 in SI); T_P is related to the duration of the unit of excess precipitation as follows:

$$T_P = \frac{\Delta t}{2} + t_{\text{lag}}, \tag{5}$$

where Δt is the excess precipitation duration (which is also the computational interval in HEC-HMS) and t_{lag} is the basin lag, defined as the time difference between the center of mass of rainfall excess and the peak of the UH.

When the lag time (t_{lag}) which is an empirical parameter is specified, HEC-HMS solves (4) and (5) to find the magnitude and time of UH peak. Given U_P and T_P, the UH can be found from the SCS-UH dimensionless, single-peaked UH. The recession model explains the drainage from natural storage in a watershed. It defines the relationship of the baseflow Q_t at any time t to an initial value Q_0 as

$$Q_t = Q_0 k^t, \tag{6}$$

where Q_0 is the initial baseflow ($t = 0$) and k is an exponential decay constant. The total flow is the sum of the direct runoff and the baseflow. Q_0 and k were all parameters identified by the historical events.

3.3. Error Estimation. The mean absolute error (MAE) was suggested by Willmott and Matsuura [28] to replace the root mean square error (RMSE) since it is a more natural definition of an average error and is unambiguous. The MAE measures the average magnitude of the errors in a set of forecasts, without considering their direction. It measures accuracy for continuous variables. The reservoir inflow directly affects the safety and the operation of a reservoir. It is thus applied in the performance measure. The difference between measured and modeled inflow is instinctively defined by the difference and the average describes the overall performance. The MAE, which ranges from zero to infinity, is defined as follows:

$$\text{MAE} = \left[T^{-1}\sum_{i=1}^{T}\left|I_i - O_i\right|\right], \tag{7}$$

where O_i is the observed inflow (m^3/s); I_i is the predicted inflow (m^3/s); i is time (hour); T is the entire evaluation time period (hour). The closer a MAE is to zero, the better the value agrees with what was observed.

The peak and cumulative inflow are important factors to evaluate the system performance. The percent error (PE) is used and defined as follows:

$$\text{PE} = \frac{\text{Simulated} - \text{Observed}}{\text{Observed}} \times 100, \tag{8}$$

where Simulated and Observed = the simulated and observed peak inflow or cumulative inflow (m^3/s).

4. Model Calibration and Validation

As mentioned earlier, this study used three methods in the HEC-HMS to simulate reservoir inflow. Three methods were SCS-CN to estimate precipitation excess, SCS-UH to calculate direct runoff, and recession to identify base flow. Therefore, the process involved tuning of CN value, percentage of impervious surface, lag time, initial discharge, recession constant, and ratio-to-peak. For the model calibration and validation, three typhoons in 2008, namely Jangmi (type 2), Sinlaku (type 2), and Fungwong (type 3), were used. The observed peak flows were 2,532, 3,260, and 1,555 m^3/s. The comparison of the temporal distribution with the observation is shown in Figure 4 (the parameter set is listed in Table 2). The MAEs were 101 m^3/s for Jangmi (model calibration), 225 m^3/s for Sinlaku (model validation), and 85 m^3/s for Fungwong (model validation). The PEs were −5.2, −7.4, and 4.9 percent in the peak inflow and −14.4, −4.4, and −14.1 percent in cumulative inflow. These results prove that the calibrated HEC-HMS model provides confident estimations for the timing and value of the peak flow and for the cumulative water volume into the reservoir. There is always a concern that the single event-based parameters are not applicable to different events. However, the calibration and validation

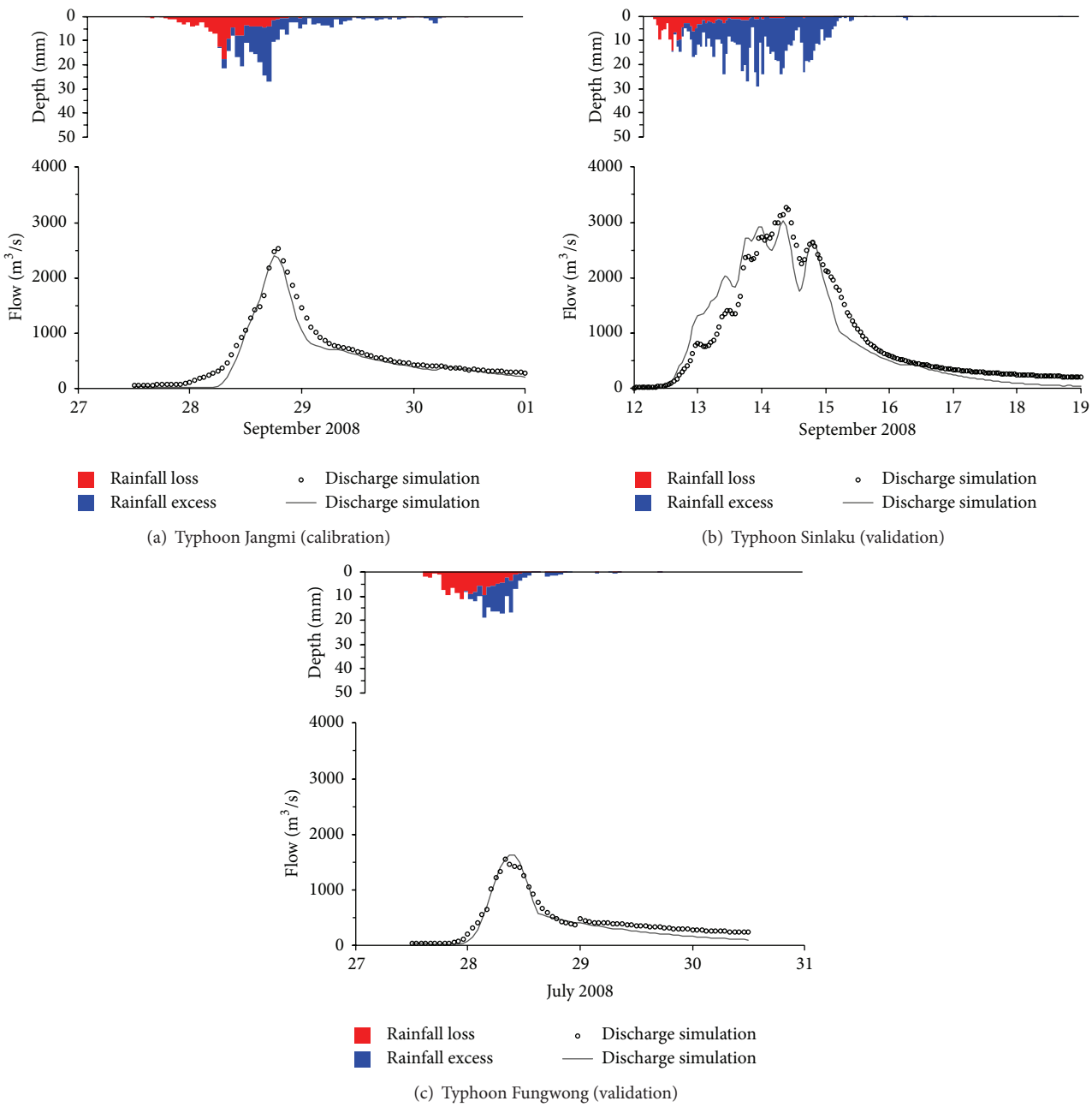

Figure 4: Observed and simulated hydrographs during (a) Typhoon Jangmi, (b) Typhoon Sinlaku, and (c) Typhoon Fungwong. The MAEs of model calibration and validation were 101.0, 224.8, and 84.8 m^3/s. The result proves that the calibrated HEC-HMS model provides confident estimations for the timing and value of the peak flow and for the cumulative water volume into the reservoir. The SCS-CN method was selected to estimate rainfall loss, including interception, depression storage, infiltration, evaporation, and transpiration. This method estimates precipitation excess as a function of cumulative precipitation, soil cover, land use, and antecedent moisture.

processes minimized the uncertainty. The comparisons of different events indicated that the parameter set is applicable for different extreme typhoon events. For the typhoons of application below, the observed inflow was at the reservoir, instead of the Hsiayun station. The verified model parameters obtained here were adopted for the applications below, but the catchment area and the lag time were adjusted to 761.05 km^2 and 250 minutes to match the difference of catchment area between the Hsiayun catchment and the Shihmen catchment (Table 2).

5. Applications

The one-way-coupling system, providing 72 h reservoir inflow forecasts, was applied to three typhoons, namely,

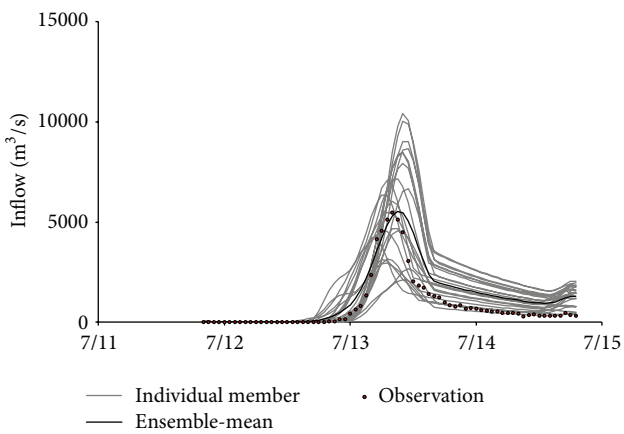

Figure 5: Example of 72 h reservoir inflow ensemble forecast for the Shihmen Reservoir from 20:00, July 11, 2013 to 19:00, July 14, 2013. This result was based on the TAPEX 78 h precipitation ensemble forecast from 14:00, July 11, 2013 to 19:00, July 14, 2013. The initial six hours were set as the warm-up time of simulation and were not included in the analysis. In addition, the gray lines represented hourly inflow forecast by each individual member. The black line represented the result by ensemble-mean of these 21 members.

Table 2: Calibrated parameter values. The same parameters set was adopted in the HEC-HMS model, but the area and the lag time, due to the difference of area between the Hsiayun catchment and the Shihmen Reservoir catchment, were adjusted from 605.29 to 761.05 km^2 and from 220 to 250 min, respectively.

Parameters	Value
Area (km^2)	
Hsiayun (1140H054)	605.29
Shihmen Reservoir	761.05
CN	68.44
Percentage of impervious surface (in percent)	0 %
Lag time (min)	
Hsiayun (1140H054)	220
Shihmen Reservoir	250
Initial discharge (m^3/s)	39.34
Recession constant	0.4
Ratio-to-peak (m^3/s)	0.35

Morakot (2009), Saola (2012), and Soulik (2013). TAPEX initially included ten plus ensemble members in 2010 and continues to increase the number of members because of advancing computer technology. To date, there are more than 20 ensemble members included in the run for precipitation forecasting. Therefore, the number of members for applied events varies. There were 13 members for Morakot, 16 members for Saola, and 22 members for Soulik applied in this study. In addition, computing technology has allowed the length of forecasts to increase. TAPEX provided only 72 h ensemble quantitative precipitation forecast for Morakot, but 78 h for Saola and Soulik. The initial six hours were set as the warm-up time of simulation and were not included in the analysis. It is noted that the forecasted length of reservoir inflow then became 66 h for Morakot and 72 h for Saola and Soulik. For example, Figure 5 shows an example of a 72 h reservoir inflow ensemble forecast from 20:00, July 11, 2013 to 19:00, July 14, 2013, based on a 78 h precipitation ensemble forecast from 14:00, July 11, 2013 to 19:00, July 14, 2013. A member produced a forecast and is shown as a grey line in the figure (individual member). The average of all members' inflows is the black line (ensemble-mean). It shall be noted that the calculation of ensemble-mean is on the hydrological part. Figure 5 shows that forecasted inflows of all members vary and cover a wide range. The magnitude and timing of the peak flows are from 2,122 to 10,395 m^3/s and from 05:00 to 11:00, respectively. The observations are shown as dots in the figure. The variation in forecasting results shows the uncertainties of using individual member and the observation is within the ensemble forecasts. Below is the detailed description for the studied typhoons.

Table 3: Selected precipitation gauges with hourly data records and the corresponding weights of Thiessen's polygon, W_n. The average rainfall of the Shihmen Reservoir catchment was calculated using Thiessen's polygon method by (1).

ID	Location		Elevation	Weights by Thiessen's polygon*
	X	Y	(m)	
21C050	273451	2745098	255	4.32
21C070	289171	2731177	1220	7.31
21C080	285756	2734043	620	9.29
21C090	289656	2726340	1260	10.02
21C140	286070	2743033	350	17.03
21D150	279651	2728316	780	9.34
21D160	275537	2720438	1620	11.52
21D170	280236	2718811	1630	12.74
21D350	286024	2713155	2000	14.46
21U110	297235	2727446	1150	3.97

*Data from the Shihmen Reservoir Management Center (http://www.wranb.gov.tw/).

5.1. Type 2 Typhoons: Soulik (2013) and Saola (2012). The CWB issued land warnings for Soulik from 20:30, July 11 to 23:30, July 13, 2013. A total of 409 mm rainfall was observed and the peak inflow was 5,458 m^3/s at 08:00, July 12. Figure 6(a) shows the error evaluation results using TAPEX's forecasts from 08:00, July 11 to 20:00, July 12. Each of individual members has its own reservoir inflow forecast. In addition, the ensemble-mean forecast was the mean of all individual member inflow forecasts. The average MAE of the ensemble-mean forecasts of seven TAPEX forecasts was 530 m^3/s. Two out of 23 members had better performances than the ensemble-mean, namely, M01 and M12. Their average MAEs were 466 and 523 m^3/s, respectively. In terms of the percentage of observed peak inflow, the MAEs of forecasted inflow ranged from 8.5 to 19.4 percent. The land warnings for Saola, a total of 66 h, were issued from 20:30, July 31 to 14:30, August 3. A total of 604 mm rainfall was reported

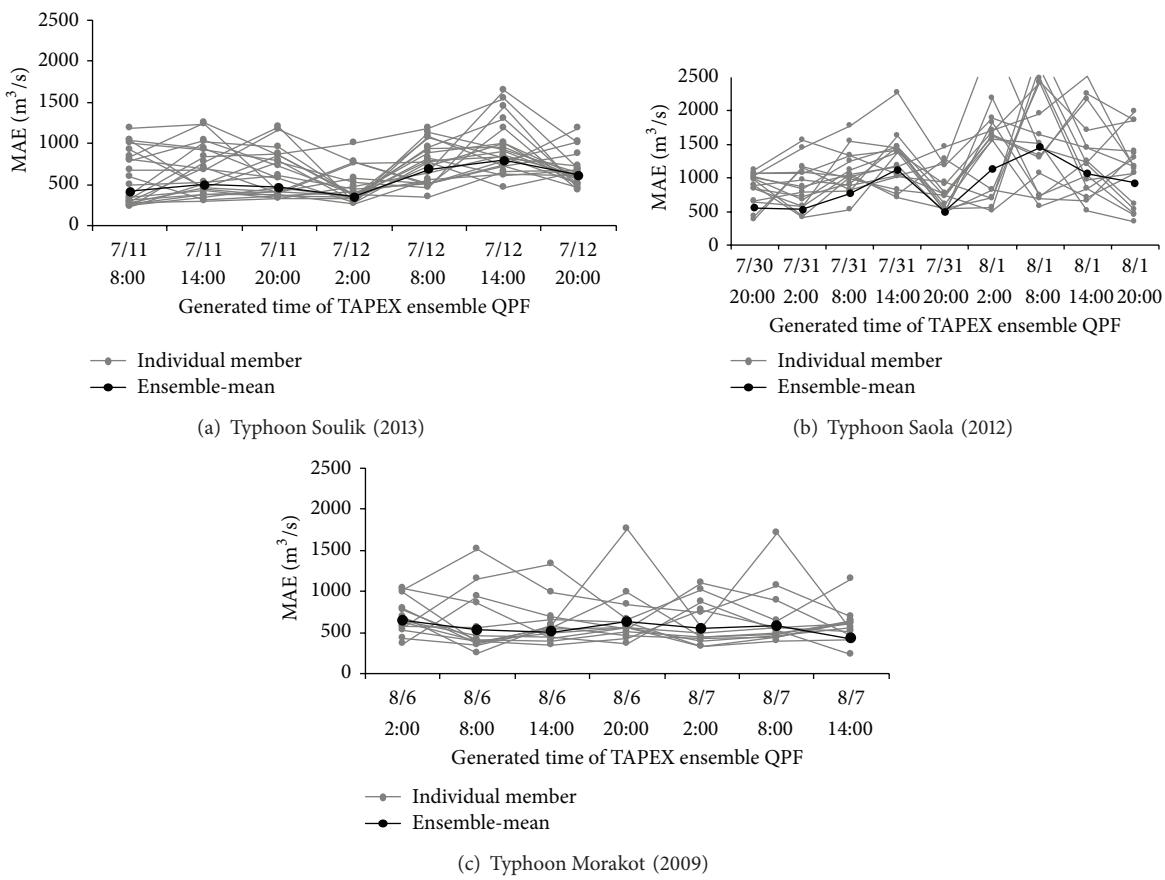

Figure 6: The evaluation of MAE. The average MAEs of the ensemble-mean was 530, 985, and 503 m^3/s for Typhoon Soulik, Typhoon Saola, and Typhoon Morakot, respectively. The performance of the ensemble-mean is probably not the best, but we cannot know which individual member is the best before it actually occurs.

and the peak inflow was 5,385 m^3/s at 07:00, August 2. Due to a longer length of land warning, nine TAPEX forecasts from 20:00, July 30 to 20:00, August 1 were used and the calculated MAEs are seen in Figure 6(b). The average MAE of the ensemble-mean was 897 m^3/s. Only M09, 827 m^3/s, had a better performance than the ensemble-mean forecast. All MAEs ranged from 15.2 to 28.2 percent in terms of the percentage of the observed peak inflow. Both Figures 6(a) and 6(b) show that the ensemble-means are located in the lower part of the plots demonstrating that using the ensemble-mean is less uncertain than randomly selecting a member's inflow.

5.2. Type 3 Typhoon: Morakot (2009). An extra application was done for Morakot, a type 3 typhoon. Morakot caused severe damages in Taiwan, and most of them were in the south. Land warnings for a total of 93 h were issued from 08:30, August 6 to 05:30, August 10. It brought a total of 398 mm rainfall on the Shihmen Reservoir catchment. The typhoon duration was long (a total of five days) so the intensity of rainfall was relatively small, leading to a low peak inflow observed to be only 1,837 m^3/s (00:00, August 7). Seven TAPEX forecasts from 02:00, August 6 to 14:00, August 7 were used and the error evaluation results are shown in Figure 6(c). The average MAE of the ensemble-mean was 557 m^3/s. A total of six members had better performances than the ensemble-mean, namely, M03, M06, M08, M09, M10, and M11. Their average MAEs were 437, 535, 520, 548, 511, and 526 m^3/s. The average MAE of all ensemble members, equal to the percentage of observed peak inflow, ranged from 23.7 to 53.5 percent. The observed peak flows of previous two typhoons were three times larger than the one of Morakot. These results show that there is higher uncertainty when using the combination of EPS and hydrological model if inflows are low. Regardless of this, using ensemble-mean, as shown in Figure 6(c), is still less uncertain than using a random member.

6. Summary and Conclusions

6.1. Uncertainty in Magnitude and Timing of Peak Flow Forecast. Figure 7 compares all members and ensemble-mean in percent between simulated and observed peak flows. Figure 8 compares the difference of timing in between simulated and observed peak flows. Listed in order of greatest magnitude and timing, the performances of peak flow forecasts were as follows: typhoon Soulik (2013), typhoon Saola (2012), and typhoon Morakot (2009). The average differences of the

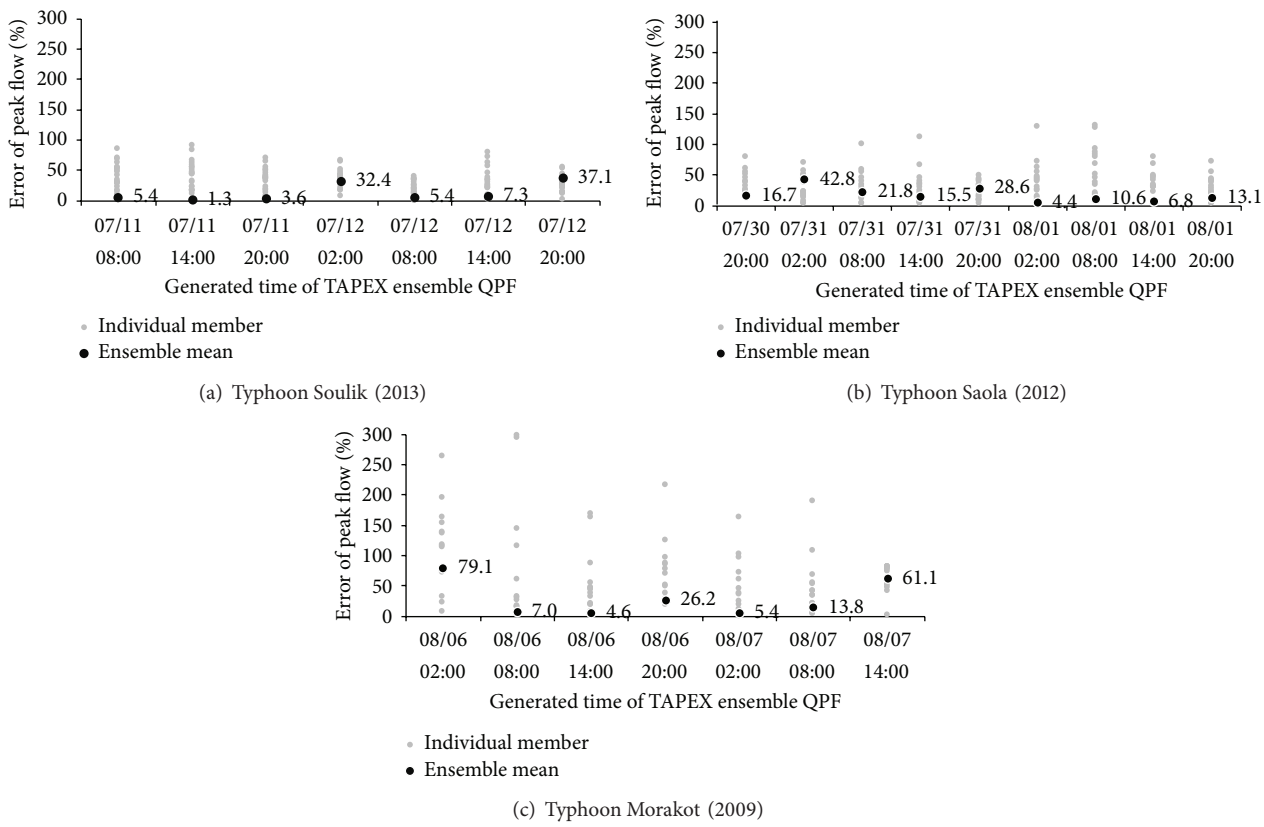

Figure 7: The error of peak flow forecast in magnitude. The averages of the ensemble-mean forecast error were 13.2, 17.8, and 28.2 percent.

ensemble-mean forecast were 13.2, 17.8, and 28.2 percent in magnitude and 0.57, 6.78, and 18.71 h in time lag. Figure 9 shows all MAEs as a box-percentile plot. The full range of variation decreases by time: the smaller the variation, the more consistent the forecasts. Two reasons may explain that (i) type 2 typhoons had heavier rainfall than type 3 typhoons and the combination of EPS and HEC-HMS performed better in heavier rainfall events and (ii) as mentioned earlier, the number of members of TAPEX increased by time, and this increased forecast accuracy. There are only limited data available since TAPEX started in 2010. More events are needed to confirm the findings when available. The MAEs of ensemble-mean are added in Figure 9 as cross marks. For the events of type 2, the cross marks are located between the minimum value and 25th percentile. For the event of type 3, the cross mark are located between the 25th and 50th percentiles. It was noted that the members with the best performance were not constant during different typhoons: M01 for Soulik, M02 for Saola, and M03 for Morakot. So far, the rule to select the best member for corresponding tracks is uncertain. This study found that the average performances of ensemble-mean were consistently located at the lower part of forecasts (Figures 6 and 8). For operational consideration, it is recommended to use the more certain ensemble-mean over the individual member.

6.2. Cumulative Length of Time. To operate a reservoir, not only the magnitude and timing of the peak flow but also the total inflow needs to be taken into account. The operators can estimate the impact of the event and operate the reservoir with precaution according to the forecasted cumulative inflow. Since TAPEX provides 72 h of precipitation forecasts, this study calculated the cumulative inflow in terms of a total of 6, 12, 18, . . . , 72 h and compared with the observations shown in Figure 10. All model runs for the three applications were included. The shaded area was bounded by the largest and smallest difference among the observations. The maximum difference between simulated and observed inflows ranged from 179.1 percent (36 h) to 52.3 percent (48 h). The bounded area significantly shrunk after 42 h, as did the forecast uncertainty. The average maximum differences were 125.4 percent before 42 h and 62.3 percent after 42 h of forecast. When the length of cumulative time is longer than 42 h, the uncertainty is half of the uncertainty for less cumulative time. It is implied that the cumulative time more than 42 h can cover the period of major typhoon rainfall. In other words, the average impact duration of a typhoon in Taiwan is 73.68 h [4], but major typhoon rainfall may occur within 42 h before and after landfall. Furthermore, if the major typhoon rainfall does not occur within the 36 h, the total inflow is insignificant and consequently amplifies

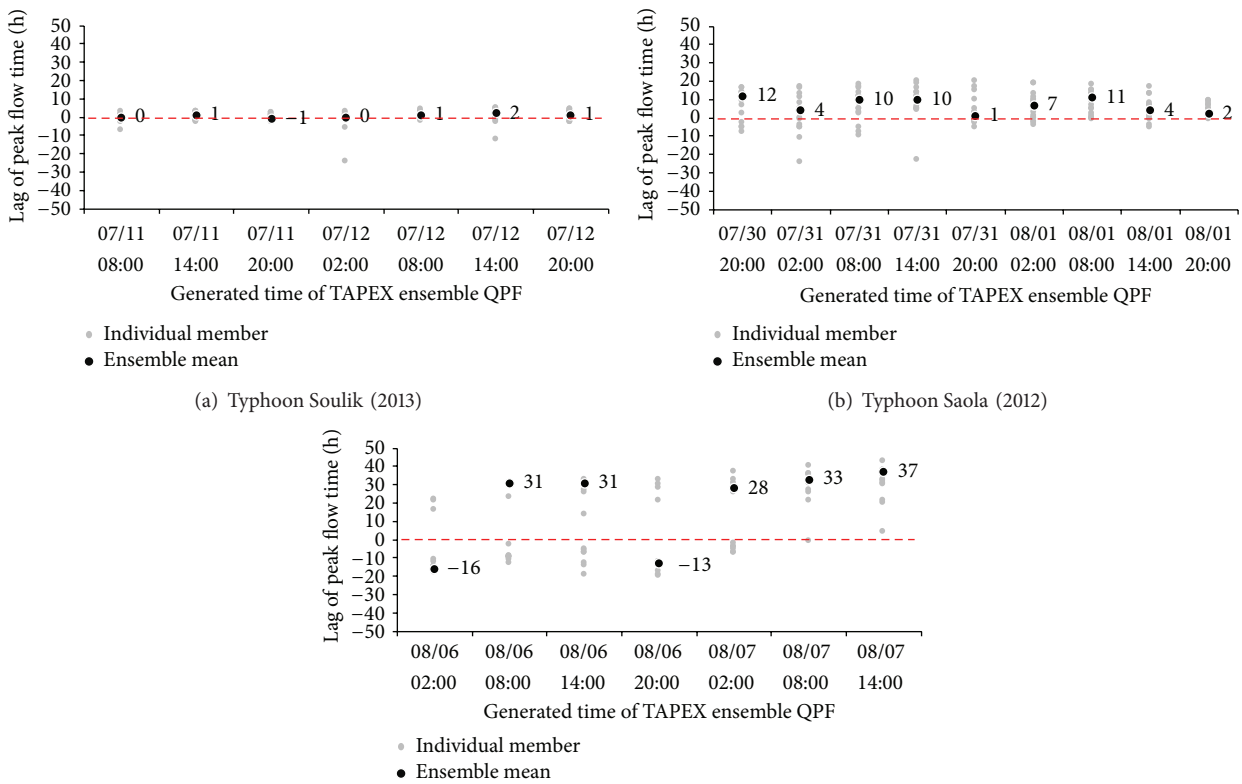

Figure 8: The error of peak flow forecast in timing. The averages of the ensemble-mean forecast error were 0.57, 6.78, and 18.71 h in time lag.

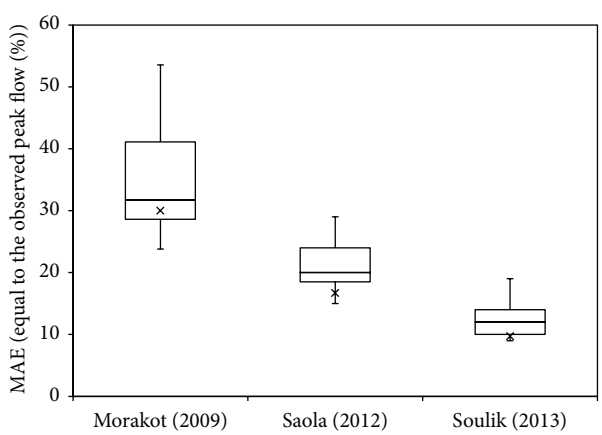

Figure 9: The box-percentile plots of MAE for the comparison of ensemble-mean (cross make) and all members (box percentile).

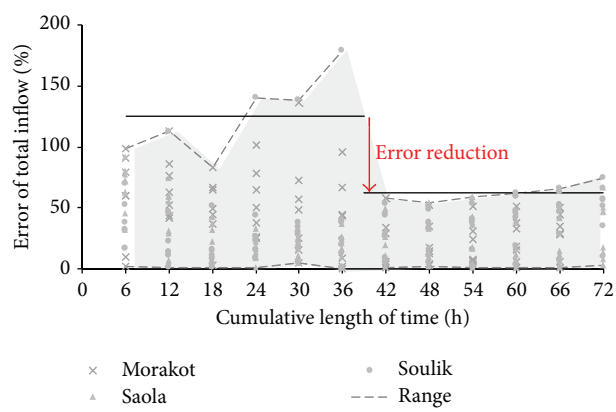

Figure 10: The error of total inflow forecast for three applications in function of cumulative length of time. The maximum of the error of total inflow varied from almost zero to 179 percent and can be reduced significantly when the cumulative length of time is larger than 42 h.

the error. The high uncertainty caused the applicability of the system to decrease with shorter length of cumulative time. Thus it is recommended to use the combination of EPS and HEC-HMS for inflow forecasts of longer cumulative time.

In conclusion, the results show that the proposed hydrometeorological system including NWPs and a hydrological model at catchment-scale shows a promising potential to serve as a valuable reference for optimal reservoir operations during extreme events. The system can provide convinced forecasts if the uncertainty of rainfall forecast and the length of lead time are well considered. More events and different study areas to implement the system should be included in the future works to test the findings in this study.

Conflict of Interests

The authors declare that there is no conflict of interests regarding the publication of this paper.

Acknowledgments

The authors acknowledge support from Taiwan Typhoon and Flood Research Institute, National Applied Research Laboratories to provide Taiwan Cooperative Precipitation Ensemble Forecast Experiment results. The authors also wish to thank two anonymous reviewers and Editor Dr. Hann-Ming H. Juang for useful comments on the paper.

References

[1] C. Lee, H. Ho, K. T. Lee et al., "Assessment of sewer flooding model based on ensemble quantitative precipitation forecast," *Journal of Hydrology*, vol. 506, pp. 101–113, 2012.

[2] M. Li, M. Yang, R. Soong, and H. Huang, "Simulating typhoon floods with gauge data and mesoscale-modeled rainfall in a mountainous watershed," *Journal of Hydrometeorology*, vol. 6, no. 3, pp. 306–323, 2005.

[3] C. L. Cheng and J. W. Liao, "Current situtation and sustainability of water resource in Taiwan," in *Proceedings of 1st Asian Water Saving Coouncil Conference*, pp. 141–148, 2011.

[4] J. Huang, C. Yu, J. Lee, L. Cheng, T. Lee, and S. Kao, "Linking typhoon tracks and spatial rainfall patterns for improving flood lead time predictions over a mesoscale mountainous watershed," *Water Resources Research*, vol. 48, pp. 1–15, 2012.

[5] C. Cheng, K. Chau, Y. Sun, and J. Lin, "Long-term prediction of discharges in Manwan Reservoir using artificial neural network models," in *Advances in Neural Networks-ISNN 2005*, vol. 3498 of *Lecture Notes in Computer Science*, pp. 1040–1045, Springer, Berlin, Germany, 2005.

[6] C. L. Wu, K. W. Chau, and Y. S. Li, "Predicting monthly streamflow using data-driven models coupled with data-preprocessing techniques," *Water Resources Research*, vol. 45, no. 8, Article ID W08432, 2009.

[7] M. Valipour, M. E. Banihabib, and S. M. R. Behbahani, "Comparison of the ARMA, ARIMA, and the autoregressive artificial neural network models in forecasting the monthly inflow of Dez dam reservoir," *Journal of Hydrology*, vol. 476, pp. 433–441, 2013.

[8] Y. Liu and H. V. Gupta, "Uncertainty in hydrologic modeling: toward an integrated data assimilation framework," *Water Resources Research*, vol. 43, no. 7, Article ID W07401, 2007.

[9] R. Hostache, P. Matgen, A. Montanari, M. Montanari, L. Hoffmann, and L. Pfister, "Propagation of uncertainties in coupled hydro-meteorological forecasting systems: a stochastic approach for the assessment of the total predictive uncertainty," *Atmospheric Research*, vol. 100, no. 2-3, pp. 263–274, 2011.

[10] M. Zappa, S. Jaun, U. Germann, A. Walser, and F. Fundel, "Superposition of three sources of uncertainties in operational flood forecasting chains," *Atmospheric Research*, vol. 100, no. 2-3, pp. 246–262, 2011.

[11] A. Rossa, K. Liechti, M. Zappa et al., "The COST 731 action: a review on uncertainty propagation in advanced hydro-meteorological forecast systems," *Atmospheric Research*, vol. 100, no. 2-3, pp. 150–167, 2011.

[12] T. N. Palmer, "A nonlinear dynamical perspective model error: a proposal for non-local stochastic-dynamic parametrization in weather and climate prediction models," *Quarterly Journal of the Royal Meteorological Society*, vol. 127, no. 572, pp. 279–304, 2001.

[13] D. S. Wilks, *Statistical Methods in the Atmospheric Sciences*, Elsevier, Amsterdam, The Netherlands, 2006.

[14] E. N. Lorenz, "The predictability of a flow which possesses many scales of motion," *Tellus*, vol. 21, pp. 289–307, 1969.

[15] H. L. Cloke and F. Pappenberger, "Ensemble flood forecasting: a review," *Journal of Hydrology*, vol. 375, no. 3-4, pp. 613–626, 2009.

[16] N. Van Steenbergen and P. Willems, "Rainfall uncertainty in flood forecasting: Belgian case study of Rivierbeek," *Journal of Hydrologic Engineering*, 2014.

[17] J. Knighton, E. White, E. Lennon, and R. Rajan, "Development of probability distributions for urban hydrologic model parameters and a Monte Carlo analysis of model sensitivity," *Hydrological Processes*, 2013.

[18] R. L. Wilby and I. Harris, "A framework for assessing uncertainties in climate change impacts: low-flow scenarios for the River Thames, UK," *Water Resources Research*, vol. 42, no. 2, Article ID W02419, 2006.

[19] N. W. Arnell, "Uncertainty in the relationship between climate forcing and hydrological response in UK catchments," *Hydrology and Earth System Sciences*, vol. 15, no. 3, pp. 897–912, 2011.

[20] J. Teng, J. Vaze, F. H. S. Chiew, B. Wang, and J. Perraud, "Estimating the relative uncertainties sourced from GCMs and hydrological models in modeling climate change impact on runoff," *Journal of Hydrometeorology*, vol. 13, no. 1, pp. 122–139, 2012.

[21] L. F. Hsiao, M. J. Yang, C. S. Lee et al., "Ensemble forecasting of typhoon rainfall and floods over a mountainous watershed in Taiwan," *Journal of Hydrology*, vol. 506, pp. 55–68, 2013.

[22] S. S. Shih, S. C. Yang, and H. T. Ouyang, "Anthropogenic effects and climate change threats on the flood diversion of Erchung Floodway in Tanshui River, Northern Taiwan," *Natural Hazards*, vol. 73, no. 3, pp. 1733–1747, 2014.

[23] Q. Zhou, G. Liu, and Z. Zhang, "Improvement and optimization of thiessen polygon method boundary treatment program," in *Proceedings of the 17th International Conference on Geoinformatics*, pp. 749–753, August 2009.

[24] D. Halwatura and M. M. M. Najim, "Application of the HEC-HMS model for runoff simulation in a tropical catchment," *Environmental Modelling and Software*, vol. 46, pp. 155–162, 2013.

[25] A. A. El Hassan, H. O. Sharif, T. Jackson, and S. Chintalapudi, "Performance of a conceptual and physically based model in simulating the response of a semi-urbanized watershed in San Antonio, Texas," *Hydrological Processes*, vol. 27, no. 24, pp. 3394–3408, 201.

[26] USACE, "Hydrologic modeling system," HEC-HMS Technical Reference Manual CPD-74B, Hydrologic Engineering Center, Davis, Calif, USA, 2000.

[27] USACE, *Hydrologic Modeling System HEC-HMS v3.5, User's Manual*, US Army Corps of Engineers, Hydrologic Engineering Center (HEC), Davis, Calif, USA, 2010.

[28] C. J. Willmott and K. Matsuura, "Advantages of the mean absolute error (MAE) over the root mean square error (RMSE) in assessing average model performance," *Climate Research*, vol. 30, no. 1, pp. 79–82, 2005.